PHYSICAL REVIEW
LETTERS

VOLUME 57 21 JULY 1986 NUMBER 3

Patterns Produced by Precipitation at a Moving Reaction Front

G. T. Dee
Central Research and Development Department, E. I. du Pont de Nemours & Company,
Experimental Station, Wilmington, Delaware 19898
(Received 16 January 1986)

Many precipitation patterns are associated with the formation of a sparingly soluble product at a moving reaction front. This paper describes a model which describes the transport, reaction, nucleation, and droplet-growth kinetics of the processes involved. It is established that the rapid change in the nucleation rate as a function of the supersaturation is essential for pattern formation. The model allows us to correlate details of the patterns with the various kinetic processes.

PACS numbers: 05.70.Fh

Systems that exhibit pattern formation are common in nature. In many systems a pattern is formed in the wake of a moving front or interface. Directional solidification[1] and front propagation into an unstable state[2] are examples of processes of this type. The pattern formation results from the steady-state morphology of the solidification interface in the former case and from the dynamic properties of the moving front in the later example. The precipitation pattern formed in the wake of a moving reaction front is another example of this later type. This phenomenon is more commonly called Liesegang band formation.[3] The process is believed to be responsible for the precipitation patterns observed in polymer films,[4] agate rocks,[5] and many other systems. Theoretically, there has been disagreement as to the mechanism responsible for these patterns. My aim here is to construct a realistic model of this system which explains all the global features of this process. The model illustrates a class of problems where "feedback" between two kinetic processes is responsible for the patterns observed.

A large quantity of experimental literature exists on this subject.[6] A number of these systems are of the type illustrated in Fig. 1. A test tube with a uniform concentration B_0 of silver nitrate ($AgNO_3$) in an aqueous gel occupies the region $x > 0$. The gel insures that no fluid flow occurs. At time $t = 0$ the region $x < 0$ contains an aqueous solution of acid, HCL say, with a uniform concentration A_0. These two substances react to produce silver chloride (AgCl) whose equilibrium concentration in the gel is C_0. If $A_0 >> B_0$ a reaction front will form at $x = 0$ and then diffuse into the gel. If the concentrations of A_0 and B_0 are chosen so that the system is initially highly supersaturated at $x = 0$ then AgCl will precipitate out of solution at the front. Under these conditions precipitation patterns are formed with the general features as shown in Fig. 1. With this experimental geometry the pattern is one dimensional. The dark bands denote the presence of precipitate. Initially, a continuous region of precipitate forms. Then bands are observed to form. If X_n, T_n, and W_n denote the position, time of formation, and width of the Nth band, respectively, then the following general observations[6,7] have been made on systems of this type. (a) It is observed that the ratios $P_n = X_{n+1}/X_n$ and $Q_n = X_n^2/T_n$ approach constant values as N in-

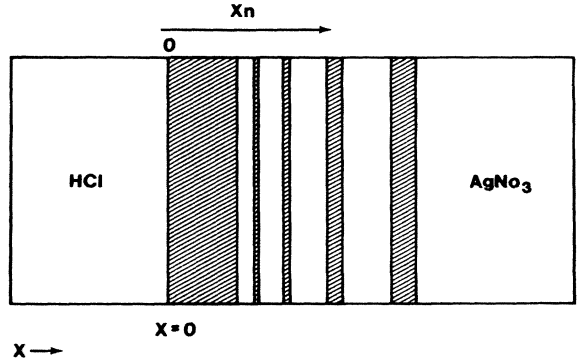

FIG. 1. A typical precipitation pattern.

creases. (b) W_n increases linearly with X_n. (c) A low density of precipitate has been detected between the bands and ahead of the forming pattern. (d) The number of bands observed increases with an increase of either A_0 or the value of the initial supersaturation.

Theoretical models of this system fall into two categories. The first attributes the patterns to a feedback mechanism between the nucleation and droplet-growth kinetics. The second explains the phenomenon in terms of a post-nucleation instability. In the first category it was Ostwald[8] who first suggested that the nucleated particles at the reaction front deplete their surroundings of the reaction product which causes the local level of supersaturation to drop to the extent that little or no further nucleation occurs. As the reaction zone moves away from this region, the growing particles in the immediate wake of the front continue to deplete the reaction zone of product and hence suppress nucleation. Eventually, the concentration of product at the moving front again achieves a value where appreciable nucleation occurs. A repetition of this sequence of events would then cause patterns to form. Theoretical predictions of the pattern geometry were made by Prager[9] and by Zeldovitch, Barenblatt, and Salganik.[10] To formulate the problem into an analytically tractable form they assumed *a priori* the existence of sharp bands. They showed that for large N or at asymptotic times the ratio P_n has a constant value. The model did not permit the presence of precipitate between the bands. The bandwidth W_n was assumed to be vanishingly small. It neglected the effects, if any, of the transport kinetics of the product, the reaction kinetics, and the details of the nucleation and droplet-growth kinetics. A numerical solution[11] of a model which included a more complete description of this system did not produce banding patterns. This study, however, did not include an adequate description of the nucleation kinetics. These discrepancies have led to the formulation of other theories. Most recent among these has been a theory[12] which attributes the phenomenon to a post-nucleation droplet-coarsening instability known as the Lifshitz-Slyozov[13] instability. This is the well-known process associated with the late-stage evolution of systems undergoing first-order phase separation. Fluctuations in droplet size during the later stages of phase separation result in the growth of larger droplets at the expense of their smaller neighbors. It has been shown that such a process can produce band patterns in a system where a continuous domain of identical droplets are perturbed. However, it has not been possible to demonstrate the formation of band patterns with the properties as described above in points (a)–(d).

I will demonstrate that the pattern solutions described above can be obtained as solutions of a model based on Ostwald's ideas. The crucial feature of this particular process is the rapid change of the nucleation rate as a function of the local supersaturation. While the Lifshitz-Slyozov instability does occur in these systems, I believe that it only affects the intraband morphology at later stages of the evolution and hence plays no role in the initial formation of the patterns observed.

The dynamic processes operative in this problem are the transport kinetics of the reactants and product, the reaction kinetics, the nucleation kinetics of the product, and the subsequent growth kinetics of the precipitate particles. If a, b, and c denote the dimensionless concentrations of the reactants and product, respectively, then the equations describing the system can be written in the form

$$\partial_t a = \partial_x^2 a - \kappa ab, \tag{1}$$

$$\partial_t b = (D_2/D_1)\partial_x^2 b - \kappa ab, \tag{2}$$

$$\partial_t c = (D_3/D_1)\partial_x^2 c + \kappa ab - u, \tag{3}$$

where we are considering a one-dimensional system, and all lengths and times have been scaled with L and L^2/D_1, respectively, where L is a length of the system. D_1, D_2, and D_3 are the diffusivities of the reactants A and B and the product C, respectively. All concentrations have been scaled with A_0, i.e., the concentration of HCl at $x=0$. The first term on the right-hand side of the above equations describes the diffusive transport of the reactants and product in a homogeneous system. The second term describes the reaction which is assumed to be second order with a reaction rate parameter k, with κ denoting the scaled reaction rate kA_0L^2/D_1. The reaction is assumed to be irreversible for simplicity, though reversible reaction kinetics can be modeled if required. The last term in Eq. (3) is a nonlinear sink term which describes the depletion of product by the nucleation and droplet-growth processes.

We assume for simplicity that the nucleated particles are spherical and remain so as they grow. We assume that the particles are immobile in the gel medium and that their growth is interface-controlled. Thus, growth of the droplets by coagulation is not included. The possible effect, if any, of the electrolyte solution on the kinetic processes is ignored. With these assumptions, the number of molecules of product contained in the precipitate phase is

$$f = (4\pi/3v)\int_0^t dt'\, J(x,t')\, r^3(x,t,t'), \tag{4}$$

where J is the nucleation rate, $r(x,t,t')$ is the radius at time t of a particle which was nucleated in the past at time t', and v is the molecular volume of the product in the solid phase. Then, using the fact that $u=\dot{f}$, we have

$$u = (4\pi/3v)\{J(x,t)\, r^3(x,t,t) + 3\int_0^t dt'\, J(x,t')\, r^2(x,t,t')\, \dot{r}(x,t,t')\}, \tag{5}$$

where $r(x,t',t')=r^*$ is the nucleation radius. The functions J, r, and r^* are functions of the supersaturation s, where $s=(C-C_0)/C_0$. The nucleation rate is of the form $J(s)=\Gamma(s)N(s)$, where $N(s)$ is the number of critical nuclei and $\Gamma(s)$ is the rate at which molecules of product attach to a critical droplet. From nucleation theory we have

$$N(s)=C_0(1+s)\exp(-4\pi\sigma r^{*2}/3k_BT), \qquad (6)$$

where σ is the surface tension. The function $\Gamma(s)$ can be described approximately by

$$\Gamma(s)=(D_3/d^2)[4\pi r^{*2}dC_0(1+s)], \qquad (7)$$

where the first factor is the rate at which molecules jump to the critical droplet from a distance d away and the second factor is the number of molecules of product in a shell of thickness d about a critical droplet. The length d is taken to be of the order of twice the molecular diameter. The nucleation radius is of the form $r^*=w/\ln(l+s)$, where w is the capillary length. The dominant dependence of J on s comes from the exponential dependence of $N(s)$ on $r^*(s)$; therefore, with the exception of the dependence of $N(s)$ on $r^*(s)$ we neglect the dependence of r^* on s by setting $r^*=w$. We then obtain the following expression for the nucleation rate

$$J(s)=J_c(1+s)^2\exp\{-[s^*/\ln(1+s)]^2\}, \qquad (8)$$

where

$$s^*=\left(\frac{4\pi\sigma w^2}{3k_BT}\right)^{1/2}, \quad J_c=\frac{4\pi D_3wC_0^2}{6d}.$$

If the growth rate of the droplets is interface controlled, then an appropriate expression for the growth rate[14] is $\dot r=Gs$ where G is a constant. Using these expressions for $J(s)$ and $\dot r(s)$, we can evaluate u and hence solve the system of Eqs. (1)–(3). Knowing u and J at each point, we can compute the density of precipitate, the average number of droplets per unit volume, and the average radius of the droplets formed. The constants used in the above expressions are shown in Table I and have been obtained from various sources.[15]

For simplicity I set $c(0,t)=c(L,t)=0.0$. This boundary condition leads to a flux of product out of the gel at $x=0$, which will cause dissolution of precipitate particles in the vicinity of $x=0.0$. With these initial conditions, I solved the equations numerically. In Fig. 2 I show a plot of the precipitate density at $t\sim 27$ h. We observe that a continuous band of precipitate forms first. Some of the precipitate has redissolved as a result of the flux of c out of the gel at $x=0$. Superimposed on this continuous background is a growing density oscillation. This oscillation grows until bands are observed to form. Visually, one would observe faint bands emerging from a continuous precipitate background. Figure 3 shows the number density of nuclei. We see that there is indeed precipitate material

TABLE I. Some typical parameter values for the AgCl system.

$A_0=0.01N$, $B_0=0.01A_0$	$C_0=7.48\times10^{15}/\text{cm}^3$
$D_1=D_2=D_3=10^{-5}$ cm^2/sec	$G=10^{-7}$ cm/sec
$\sigma=170$ erg/cm^2	$r^*=w=10$ Å

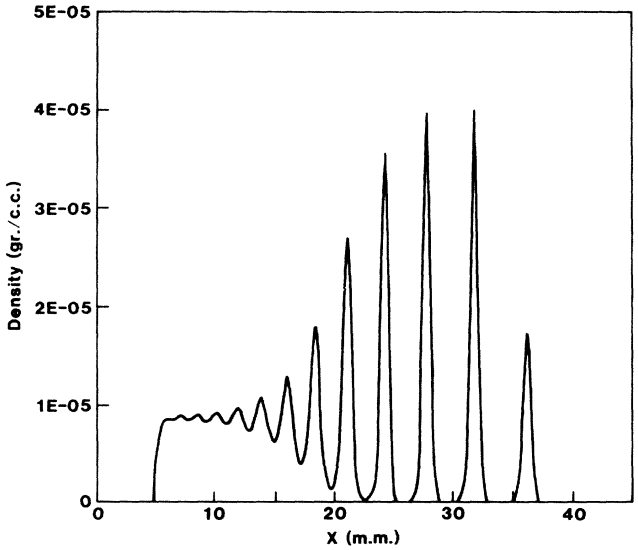

FIG. 2. A plot of the density of precipitate as a function of position at $t=27$ h and $k=10^5$ mol^{-1} sec^{-1}.

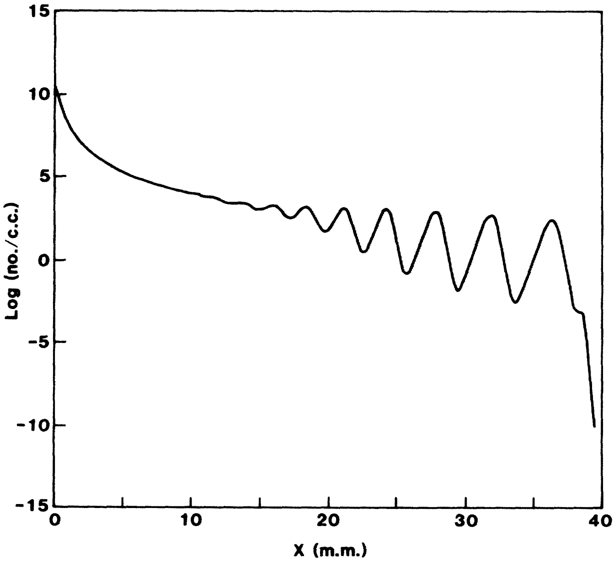

FIG. 3. A plot of the number density of precipitate particles as a function of position at $t=27$ h and $k=10^5$ mol^{-1} sec^{-1}.

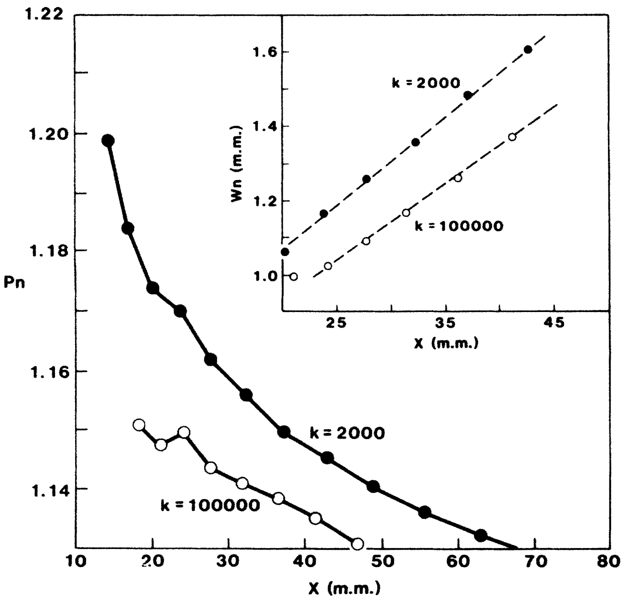

FIG. 4. A plot of the ratio P_n vs position of the bands for values of the reaction rate equal to 2000 and 100 000 mol^{-1} sec^{-1}, respectively. Inset: Plot of the bandwidth W_n for the same values of k. The noise in the data for P_n is due to numerical error.

between the bands and in front of the leading band. Figure 4 shows the ratio P_n for two different reaction rates where P_n is plotted as a function of band position. The simulation at the lower value of k was run for a longer time, which accounts for the observation of bands at larger values of x. The values of P_n for both reaction rates drift towards lower values. The extent of the drift is smaller for the larger value of the reaction rate and both sets of data indicate an asymptotic approach to a constant value. Since the variation in P_n for the larger value of k is only on the order of 1%, measurement of such an effect may be difficult. This fact may account for the large number of experimental observations which indicate a constant value of P_n. The inset in Fig. 4 shows the bandwidth W_n as a function of band position for two values of k. The bandwidth is taken to be the width at a precipitate density of 10^{-5} g/cm^3. In both cases, the bandwidth increases linearly with x. We also observe that the width at fixed x is smaller for the case of the higher reaction rate. Thus, the reaction-zone width which decreases with increasing k affects both the band spacings and the bandwidths. Since κ is proportional to A_0k, this implies that the bandwidths decrease with increasing A_0.

The model calculations imply the following conclusions: (1) The rapid change of the nucleation rate with supersaturation is essential for pattern formation.[16] (2) Precipitate exists between the bands. (3) P_n and Q_n are slowly varying functions of X_n for finite reaction rate k. (4) W_n increases linearly with X_n. (5) The number of bands observed increases with A_0 or k and their widths decrease.

I would like to thank L. Manring and S. Mazur for many helpful conversations.

---

[1] J. S. Langer, Rev. Mod. Phys. **52**, 1 (1980).

[2] G. Dee, J. Stat. Phys. **39**, 705 (1985).

[3] R. E. Liesegang, Naturwiss. Wochenschr. **11**, 353 (1896), and Photog. Archiv. **21**, 221 (1986).

[4] K. F. Mueller, Science **225**, 1021 (1984).

[5] R. A. Ball, Aust. Gemmol. **12**, 89 (1974).

[6] K. M. Piffai, V. K. Vaidyan, and M. A. Ittyachan, Colloid Polym. Sci. **258**, 831–838 (1980); K. H. Stern, *Bibliography of Liesegang Rings*, U. S. Department of Commerce Miscellaneous Publication No. 29 (U. S. GPO, Washington, D.C., 1967), 2nd ed.

[7] S. C. Muller, S. Kai, and J. Ross, J. Phys. Chem. **86**, 4078 (1982).

[8] W. Ostwald, *Lehrbuch der Allgemeinen Chemie* (Engelman, Liepzig, 1897).

[9] S. Prager, J. Chem. Phys. **25**, 279 (1956).

[10] Ya. B. Zeldovitch, G. I. Barenblatt, and R. L. Salganik, Dokl. Akad. Nauk SSSR **140**, 1281 (1962) [Sov. Phys. Dokl. **6**, 869 (1962)].

[11] G. Venzl and J. Ross, J. Chem. Phys. **77**, 1302 (1982).

[12] R. Feeney, S. L. Schmidt, P. Strickholm, J. Chadam, and P. Ortoleva, J. Chem. Phys. **78**, 1293 (1983); R. Lovett, P. Ortoleva, and J. Ross, J. Chem. Phys. **69**, 947 (1978).

[13] I. M. Lifshitz and V. V. Slyozov, J. Phys. Chem. Solids **19**, 35 (1961).

[14] M. C. Flemings, *Solidification Processing* (McGraw-Hill, New York, 1974).

[15] G. Venzl and J. Ross, J. Chem. Phys. **77**, 1308 (1982).

[16] Mel LeVan, J. Reiter, and J. Ross, private communication.